Applied Energy 266 (2020) 114741

Contents lists available at ScienceDirect

Applied Energy

journal homepage: www.elsevier.com/locate/apenergy

Participation of photovoltaic power producers in short-term electricity markets based on rescheduling and risk-hedging mapping

Agustín A. Sánchez de la Nieta[a,b,*], Nikolaos G. Paterakis[c], Madeleine Gibescu[a]

[a] Utrecht University, Utrecht, the Netherlands
[b] Loyola Institute of Science and Technology (Loyola.Tech), Universidad Loyola Andalucía, Seville, Spain
[c] Eindhoven University of Technology, Eindhoven, the Netherlands

HIGHLIGHTS

- Two models for the participation of PV power producers in three market floors.
- Rescheduling following the characteristic of the six intraday market sessions.
- Risk-hedging map associated with the scheduling and rescheduling of the bids.

ARTICLE INFO

Keywords:
Balancing market
Conditional value-at-risk
Day-ahead market
Intraday market
PV power producer
Strategic bidding

ABSTRACT

Optimal bidding that considers different electricity market floors can increase the financial gains of photovoltaic (PV) power producers. However, the current approach to trading PV power essentially consists of committing to sell the forecasted PV generation. To analyze profits and investigate new business opportunities for PV power producers, this paper proposes two novel stochastic programming-based methods for scheduling and rescheduling for trading the PV generated energy in day-ahead and intraday electricity markets. Risk-hedging is also considered in terms of co-optimizing the expected profit with the Conditional Value-at-Risk (CVaR) metric. As a consequence of the structure and organization of the market floors and due to different market windows, rescheduling is necessary to exploit the most recent information. Updated rescheduling progressively reveals actual profits or losses, risk-hedging possible engagement in business transactions, and the final effect of strategic bidding. A case study in the Spanish electricity market based on actual data is presented. The analysis of the case study shows the influence of the three market floors (day-ahead, intraday, and imbalance), the participation in multiple intraday sessions, risk-hedging, and rescheduling on the profits of the PV producer.

1. Introduction

Electricity consumption is intrinsically associated with industrial development and societal prosperity. Following a century of heavy reliance on fossil fuels, the electric power industry is currently undergoing a paradigm shift to utilizing more sustainable alternatives. Given the environmental impact of the electricity sector, the Kyoto protocol [1] was signed by several countries as they committed to reducing greenhouse gas (GHG) emissions from conventional power plants and other sources. With the approval of the first agreement in 1997, the energy transition to more sustainable energy systems was initiated. The energy transition in the electricity sector is characterized by the increasing adoption of renewable energy sources. Wind power has been the leading source of renewable energy production due to the maturity of the relevant technology. The focus now is on the proliferation of photovoltaic (PV) power, which is regarded as a real instrument towards a sustainable power system; this is because it can be generated on a large scale and locally, i.e., closer to the end user.

The success of the energy transition largely depends on the existence of viable business cases for renewable power generation and storage technologies in a deregulated market environment. Two mechanisms have traditionally been used to encourage the deployment of renewable energy installations: feed-in tariffs, or a feed-in premium on top of the day-ahead electricity market prices.

However, the global financial crisis has led to reductions in premium payments, increasing the uncertainty of this income stream.

* Corresponding author.
E-mail addresses: a.a.sanchezdelanietalopez@uu.nl, aasanchez@uloyola.es (A.A. Sánchez de la Nieta), N.Paterakis@tue.nl (N.G. Paterakis), M.Gibescu@uu.nl (M. Gibescu).

https://doi.org/10.1016/j.apenergy.2020.114741
Received 18 September 2019; Received in revised form 1 February 2020; Accepted 24 February 2020
Available online 26 March 2020
0306-2619/

Another option for renewable energy producers is to trade energy in electricity markets. Interestingly, despite the significant reduction in premium payments, PV power producers still prefer premium income over the income from selling PV production in electricity markets, because the risk associated with the premium income is lower than the risk of participating in short-term electricity markets. The main reason for this is that PV power producers mostly rely on simple heuristics to trade their forecasted PV generation.

Sustainability is becoming a priority for companies around the world and is transforming into a social movement that also has financial implications. In 2014, the RE100, a global corporate initiative of industries committing to cover their energy requirements by renewable energy, was launched [2]. The new energy culture brought the growth of Power Purchase Agreements (PPAs) or bilateral contracts. There are different types of PPAs, such as the On-site PPA, the Sleeved PPA, and the Virtual PPA. PPAs are the current alternative to wholesale markets, premiums, and extra-payments. The added value of securing a PPA for a PV project is increased bankability, because the certainty of future cash flows is guaranteed. As a result, PPAs have boosted the development of PV projects. Nonetheless, risk-hedging remains the instrument for managing financial risks when the PV power producer participates in the wholesale electricity market [3].

To improve the actual PV power trading process, two novel risk-aware models are proposed in this paper for scheduling and re-scheduling to bid the PV production in the day-ahead and intraday markets based on stochastic mixed-integer linear programming re-scheduling models (SMILP-RSM). As a consequence of the structure of the considered day-ahead and intraday markets (i.e., the Spanish electricity market [4]), the decision process of scheduling for both markets is not sufficient to mitigate the uncertainty. By the time an intraday session opens, the day-ahead market prices are known with certainty and there is less uncertainty in anticipating the future PV production as the look-ahead time decreases.

Consequently, rescheduling for the different intraday market windows will reveal the real profits or losses, risk-hedging, and the final effect of strategic bidding on profits. Considering the objectives of maximizing the expected profit and optimizing the risk metric, PV generation can be traded in day-ahead and intraday electricity markets. The balancing market mechanism is used to penalize the imbalances of the PV power producer. For the analysis of the two SMILP-RSMs, a test case based on the organization and data of the Spanish electricity market shows the influence of the three market floors, the risk-hedging, and the actual rescheduling for minimizing the imbalance penalties. The Spanish intraday electricity market has six sessions with different time frames. Because of these different time frames, several models with, and without, consideration for the intraday electricity market allow the evaluation of the effects on the expected profit for the whole day-ahead scheduling, rescheduling, and final profits.

1.1. Literature review

The fact that PV is a clean power generation technology makes it relevant for energy transition [5]. With zero CO_2 emissions, PV technology is spearheading decarbonization through different approaches to the integration of PV power in modern power systems. Some examples of such approaches are microgrids [6] coupled with energy storage systems, residential sector applications [7], prosumption [8], industrial sector applications, support of electric vehicles [9], peer-to-peer electricity trading [10], premiums and optimization of portfolios of renewable energy sources [11], utility-scale Solar PV projects [12], and electricity market participation [13]. Several studies investigated the market value and cost of PV electricity production [14] and the merit order effect of PV on wholesale electricity market prices [15,16]. The feed-in tariff system for PV producers in Germany was analyzed in [17], while a similar subject focusing on China was discussed in [18,19]. Apart from the feed-in tariff system, the effect of other mechanisms such as renewable portfolio standards and renewable energy certificates have also been studied [20,21].

To the best of the authors' knowledge [13] is the first study in which stochastic programming was used to develop a day-ahead market participation strategy for PV producers, also taking the balancing market into account as a penalization mechanism. Following the approach that was presented in [13], other authors conducted further studies in the field of PV trading in electricity markets. Some new contributions were presented in [22], in which virtual bidding was included along with risk hedging. A similar approach to [13] was presented in [23], but the PV trading optimization algorithm is similar to the methodology proposed in [24], without considering risk hedging. Most relevant studies in the literature consider wind power instead. There are several studies in which risk-aware day-ahead market trading models for wind [24] and combined wind and hydro-pump power plants [25] were based on stochastic programming. Also, medium-term planning was considered in [26]. From an operational perspective, risk is typically considered via the Conditional Value-at-Risk (CVaR) [27]. Without the consideration of CVaR, an optimal wind-PV coordinated bidding strategy shows the effect of a single bid for uncertain wind and PV power production [28]. The participation of a wind farm coupled with energy storage in multi-stage electricity markets was studied in [29] using dynamic programming. Also, a rolling optimization model for trading the energy of a wind farm coupled with energy storage in day-ahead and intraday markets was presented in [30] without considering risk hedging or rescheduling. Nonetheless, aggregators could also re-schedule distributed energy sources for market participation as proposed in [31].

Apart from the development of uncertainty and risk-aware market participation strategies, financial instruments can also be used to manage risks. For example, PPAs can be perceived to be risk free [32]. Other instruments including bilateral contracts [33] and options [3,34,35] can be used to partly mitigate financial risks. A risk-aware model for day-ahead market participation considering bilateral contracts was proposed in [33]. A multi-stage stochastic optimization model was used to determine an optimal strategy to sell the energy of a risk-averse producer considering options, forward contracts, and pool market trading in [3]. A market-specific seasonal trading behavior in NASDAQ OMX electricity options was analyzed in [36]. Some energy options were described in [37,38] studied the trading of wind power through physically settled options and short-term electricity markets.

Another option for managing the uncertainty in PV production is to participate in intraday markets. Trading energy in the intraday market gives the opportunity to raise additional revenue and reduces imbalances between the total sale/purchase bids and production. The trading of wind power with storage was studied in [39] with a short-term horizon; however, a two-stage stochastic programming problem was proposed to optimize the participation of the wind and storage in the pool market, composed of the day-ahead market, an intraday session, and the balancing market. The stochastic model was implemented as a stochastic convex optimization problem. To benefit from the Elbas intraday market, a simple algorithm was developed in [40], considering the Elspot day-ahead, Elbas intraday, and regulation power markets. Adaptive trading in the continuous intraday electricity market for a storage unit was introduced in [41], modeling the problem through a Markov decision process framework. The effect of the intraday in the balancing market was explored in [42] in balancing Germany's electricity system. With a long-term horizon, an annual techno-economic analysis of a PV solar power plant with storage systems was conducted in [43]. The economic analysis considered the day-ahead and intraday markets and secondary reserve, as well as the balancing market. In this case, market participation was represented through a linear-programming-based model predictive control approach [44].

1.2. Aims and contributions

This paper proposes and compares two short-term market

participation models: i) the independent optimal bidding of a PV power producer in the three market floors (SMILP-RSM-1); and ii) the optimal bidding of a PV producer in which the scheduling and rescheduling process reach all forward decisions in the three market floors (SMILP-RSM-2). The scheduling and rescheduling optimization processes depend on the number and timing of the intraday market sessions. Via rescheduling, recent information on the stochastic processes is considered. Mixed-integer linear programming is used to develop two-stage stochastic optimization models using a node-variable formulation.

The principal contributions of this paper are as follows:

- Two strategic bidding models (SMILP-RSM-1 and SMILP-RSM-2) for the participation of PV power producers in short-term electricity markets are proposed.
- Rescheduling following the characteristics of the intraday market sessions to consider updated information on the stochastic processes is introduced.
- The risk-hedging effect associated with the scheduling and rescheduling of the bids is mapped and analyzed.

The remainder of the paper is structured as follows: first, in Section 2 the wholesale market environment is introduced. Then, in Section 3 the mathematical models for both strategies are presented, while in Section 4 the case study and numerical results are presented and discussed. Finally, conclusions are drawn in Section 5.

2. Wholesale electricity markets

Wholesale electricity markets allow the trading of electrical energy in bulk. Different agents, such as producers, large consumers, and retailers trade energy by accessing different market structures. The European daily market is a clearing process that starts at noon on the previous day D-1 and continues for the 24 h of day D. Once the Market Operator matches the aggregate demand and supply curves of producers, consumers, and retailers, the cleared price and volume of energy are announced. The requirement for transparency in the way that electricity market prices are determined, and to achieve the target of a harmonized European electricity market, has led to the utilization of a single market-clearing tool across many countries, namely, Euphemia [45].

Due to the significant lead time between the clearing of the day-ahead market and the physical delivery of electrical energy, imbalances occur at both the production and demand sides. Market participants must balance their day-ahead market position in the balancing markets by buying their energy deficit or selling their energy surplus in the balancing market. In general, this implies that market participants face either penalties or opportunity costs in case they accept the upward or downward imbalance prices to settle their total imbalance. As a remedy, market agents can participate in intraday market sessions throughout the trading day D to reduce their final imbalance.

Despite the fact that all three aforementioned wholesale market mechanisms are generally available, their specific structure and organizational implementation differ across countries. This paper focuses on the Spanish electricity market ([4,46]), which comprises of six intraday sessions with different time frames and is also currently characterized by the proliferation of PV power capacity (see Nomenclature in Table 1).

2.1. The Spanish day-ahead market

The European prices are matched daily at 12 PM of day D-1. The Spanish day-ahead market (DA) is cleared for the 24 hourly periods of day D. Once the energy volume and price pairs are submitted to the market operator by the market participants, the former aggregates them to form the total supply and demand curves. This aggregation allows the discovery of the intersection point of both curves considering the simple orders. After that, the clearing algorithm matches the complex orders [45].

Table 1
Nomenclature.

Indices and Sets	
$i(\mathscr{I})$	Index (set) related to optimization processes
$j(\mathscr{J})$	Index (set) related to the intraday session
$s(\mathscr{S})$	Index (set) related to scenarios
$t(\mathscr{T})$	Index (set) related to periods $t = 1, 2, 3, ..., 24$
t_1	Index related to periods t_1 of the intraday window of session $j = 1$. $t_1 \subset \mathscr{T}$, $t_1 = \{1, 2, 3, ..., 24\}$
t_2	Index related to periods t_2 of the intraday window of session $j = 2$. $t_2 \subset \mathscr{T}$, $t_2 = \{1, 2, 3, ..., 24\}$
t_3	Index related to periods t_3 of the intraday window of session $j = 3$. $t_3 \subset \mathscr{T}$, $t_3 = \{5, 6, 7, ..., 24\}$
t_4	Index related to periods t_4 of the intraday window of session $j = 4$. $t_4 \subset \mathscr{T}$, $t_4 = \{8, 9, 10, ..., 24\}$
t_5	Index related to periods t_5 of the intraday window of session $j = 5$. $t_5 \subset \mathscr{T}$, $t_5 = \{12, 13, 14, ..., 24\}$
t_6	Index related to periods t_6 of the intraday window of session $j = 6$. $t_6 \subset \mathscr{T}$, $t_6 = \{16, 17, 18, ..., 24\}$
s	Index related to scenarios
Parameters	
A_n^{PV}	Area of the PV panel [m^2]
E^{MAX}	Limit of energy traded and imbalances [MWh]
G	Solar irradiance [W/m^2]
N	Total number of arrays of the PV power plant
$p_{t,s}$	PV production in period t and scenario s [MWh]
P^{PV}	PV power output of the PV panels [MW]
α	Confidence level used for CVaR
β_i	Weight for evaluation of multi-objective profit-CVaR for each i
η_n^{PV}	Efficiency of each array
$\pi_{t,s}^{-BM}$	Price of downward imbalance market in period t and scenario s [€/MWh]
$\pi_{t,s}^{+BM}$	Price of upward imbalance market in period t and scenario s [€/MWh]
$\pi_{t,s}^{DA}$	Price of day-ahead market in period t and scenario s [€/MWh]
$\pi_{t_j,s}^{IDj}$	Price of intraday session j in period t_j and scenario s [€/MWh]
ρ_s	Probability of each scenario s
Decision variables	
$B_{t,s}$	Imbalance between the production and bids in period t and scenario s [MWh]
$B_{t,s}^{-}$	Downward imbalance between the production and bids in period t and scenario s [MWh]
$B_{t,s}^{+}$	Upward imbalance between the production and bids in period t and scenario s [MWh]
$CVaR$	Conditional value-at-risk [€]
PF^{PV}	Total profits of the PV power producer [€]
$PF_{t,s}^{PV}$	Profit of the PV power producer per period t and scenario s [€]
q_t^{DA}	Bid in the day-ahead market in period t [MWh]
$q_{t_j}^{IDj}$	Bid in the intraday session j in period t_j [MWh]
VaR	Value at Risk [€]
η_s	Auxiliary variable used in CVaR evaluation per scenario s
Binary variable	
$w_{t,s}$	0/1 variable, 0 when there is an upward imbalance and 1 when is a downward imbalance

2.2. The Spanish intraday market

After the day-ahead market is cleared, market participants can access several intraday sessions to establish their positions in a similar way to the day-ahead market. The agents can manage imbalances until the corresponding session closes. Agents present their sale/purchase bids during the intraday sessions, whether they participated in the day-ahead market or executed a bilateral contract. The Spanish electricity market hosts six intraday auctions (ID1-ID6). Table 2 presents the

Table 2
Intraday market sessions [4].

	Session 1	Session 2	Session 3	Session 4	Session 5	Session 6
Opening time	17:00	21:00	01:00	04:00	08:00	12:00
Closing time	18:50	21:50	01:50	04:50	08:50	12:50
Matching process	18:50	21:50	01:50	04:50	08:50	12:50
Results publication	18:57	21:57	01:57	04:57	08:57	12:57
TSOs publication	19:15	22:15	02:15	05:15	09:15	13:15
Market window	27 h (22–24&1–24)	24 h (1–24)	20 h (5–24)	17 h (8–24)	13 h (12–24)	9 h (16–24)

Table 3
Markets, scheduling & rescheduling, and optimal and real (∗) evaluation for the set of models 1 SMILP-RSM-1.

Market/Opt.	(1st,∗)	(2nd,∗)	(3rd,∗)	(4th,∗)	(5th,∗)	(6th,∗)	(7th,∗)	(8th,∗)
DA	(✓,-)	(-,DA∗)	(-,DA∗)	(-,DA∗)	(-,DA∗)	(-,DA∗)	(-,DA∗)	(-,DA∗)
ID1	(-,-)	(✓,-)	(-,ID1∗)	(-,ID1∗)	(-,ID1∗)	(-,ID1∗)	(-,ID1∗)	(-,ID1∗)
ID2	(-,-)	(-,-)	(✓,-)	(-,ID2∗)	(-,ID2∗)	(-,ID2∗)	(-,ID2∗)	(-,ID2∗)
ID3	(-,-)	(-,-)	(-,-)	(✓,-)	(-,ID3∗)	(-,ID3∗)	(-,ID3∗)	(-,ID3∗)
ID4	(-,-)	(-,-)	(-,-)	(-,-)	(✓,-)	(-,ID4∗)	(-,ID4∗)	(-,ID4∗)
ID5	(-,-)	(-,-)	(-,-)	(-,-)	(-,-)	(✓,-)	(-,ID5∗)	(-,ID5∗)
ID6	(-,-)	(-,-)	(-,-)	(-,-)	(-,-)	(-,-)	(✓,-)	(-,ID6∗)
BM	(✓,-)	(✓,-)	(✓,-)	(✓,-)	(✓,-)	(✓,-)	(✓,-)	(-,BM∗)

timing characteristics of the six intraday market sessions.

2.3. The Spanish imbalance market

The Spanish imbalance or balancing market (BM) [47] generates an hourly upward and downward imbalance price. Generators can have either an upward or a downward imbalance volume. The generator's imbalance is calculated as the actual generator's production minus the generator's bid (1). When generators produce more energy than they submitted to all markets (excess of production), generators are said to have upward imbalances. Hence, generators earn the upward imbalance volume multiplied by the upward imbalance price, which is equal to, or lower than, the day-ahead electricity market price (2). Evidently, this constitutes an opportunity cost. In the opposite case, that is, if generators produce less energy than is bid, the total imbalance is moving in a downward direction. The downward imbalance cost is the imbalance volume multiplied by the downward imbalance price (3), which is equal to, or higher than, the day-ahead electricity market price, thus constituting an imbalance penalty.

$$imbalance = generation - bids \tag{1}$$

$$Income = price^{Upward} \cdot imbalance^{Upward} \tag{2}$$

$$Cost = price^{Downward} \cdot imbalance^{Downward} \tag{3}$$

The mathematical models that are proposed in this study optimally decide the PV energy volumes that are traded in the day-ahead, intraday, and balancing markets. These mathematical models are considered as a price taker because of the decided PV energy volumes, which are not large enough to change any of the wholesale market prices.

3. Mathematical formulation

Each strategy involves the solution of a set of optimization models, such as the proposed SMILP-RSM-1 and SMILP-RSM-2. Both sets of models have seven optimization processes; each model traded in each market and its associated window. Several market windows have real information that needs to be updated until the market window of the scheduling and rescheduling is considered. In addition, the optimal solutions of previous scheduling or rescheduling processes are also introduced during the subsequent optimization process. After rescheduling the last (sixth) intraday session, i.e., in the 7th optimization process, a post-market evaluation calculates the actual profits because all the stochastic processes have been realized.

In each optimization process, the SMILP-RSM-1 strategy provides a decision that is related only to the energy bidding of the market window of that optimization process. Therefore, these sets of decision variables can be written as: $\Phi_1 = \{q_t^{DA}\}$, $\Phi_2 = \{q_{t_1}^{ID1}\}$, $\Phi_3 = \{q_{t_2}^{ID2}\}$, $\Phi_4 = \{q_{t_3}^{ID3}\}$, $\Phi_5 = \{q_{t_4}^{ID4}\}$, $\Phi_6 = \{q_{t_5}^{ID5}\}$, and $\Phi_7 = \{q_{t_6}^{ID6}\}$, where Φ_i is related to the market bid decisions of the i-th optimization process. By contrast, the SMILP-RSM-2 strategy provides all the forward bid decisions. The sets of decision variables for this optimization model can be written as: $\theta_1 = \{q_t^{DA}, q_{t_1}^{ID1}, q_{t_2}^{ID2}, q_{t_3}^{ID3}, q_{t_4}^{ID4}, q_{t_5}^{ID5}, q_{t_6}^{ID6}\}$, $\theta_2 = \{q_{t_1}^{ID1}, q_{t_2}^{ID2}, q_{t_3}^{ID3}, q_{t_4}^{ID4}, q_{t_5}^{ID5}, q_{t_6}^{ID6}\}$, $\theta_3 = \{q_{t_2}^{ID2}, q_{t_3}^{ID3}, q_{t_4}^{ID4}, q_{t_5}^{ID5}, q_{t_6}^{ID6}\}$, $\theta_4 = \{q_{t_3}^{ID3}, q_{t_4}^{ID4}, q_{t_5}^{ID5}, q_{t_6}^{ID6}\}$, $\theta_5 = \{q_{t_4}^{ID4}, q_{t_5}^{ID5}, q_{t_6}^{ID6}\}$, $\theta_6 = \{q_{t_5}^{ID5}, q_{t_6}^{ID6}\}$ and $\theta_7 = \{q_{t_6}^{ID6}\}$, where θ_i is related to the market bid decisions of the i-th optimization process.

Tables 3 and 4 provide information about the markets that are involved in each optimization process. This information includes involved market bid decisions and updated real information. Scheduling is associated with the 1st optimization process and rescheduling occurs from the 2nd to the 7th optimization process. The columns of Tables 3 and 4 are related to the optimization process, during which the 1st scheduling refers to the day-ahead window, the 2nd to the 7th rescheduling refer to the intraday market session windows, and the 8th represents a post-market evaluation with all of the information at hand. In other words, during the 8th optimization process, all the decision variables are essentially fixed to their optimal values as they were calculated during the previous optimization processes. The post-market evaluation allows the quantification of the actual profit achieved by both strategies, hence, it is a proxy to their effectiveness. The rows of Tables 3 and 4 show the market that is involved with a checkmark (✓). Every cell shows two components inside of brackets, (market involved [yes or no], optimal solution and real information). The optimal solutions are DA∗, ID1∗, ID2∗, ID3∗, ID4∗, ID5∗, and ID6∗. The real information is related to PV production, DA prices, ID prices, and both upward and downward balancing prices. To further clarify which quantities are involved in each optimization process, Figs. 1 and 2 display the parameters and market bid variables in each optimization process.

First, the parameters that are presented in Figs. 1 and 2 are prices, PV production, and the bid that was decided during the previous market window optimization process for both strategies (the first row in

Table 4
Markets, scheduling & rescheduling, and optimal and real (∗) evaluation for the set of models 2 SMILP-RSM-2.

Market/Opt.	(1st,∗)	(2nd,∗)	(3rd,∗)	(4th,∗)	(5th,∗)	(6th,∗)	(7th,∗)	(8th,∗)
DA	(✓,-)	(-,DA∗)	(-,DA∗)	(-,DA∗)	(-,DA∗)	(-,DA∗)	(-,DA∗)	(-,DA∗)
ID1	(✓,-)	(✓,-)	(-,ID1∗)	(-,ID1∗)	(-,ID1∗)	(-,ID1∗)	(-,ID1∗)	(-,ID1∗)
ID2	(✓,-)	(✓,-)	(✓,-)	(-,ID2∗)	(-,ID2∗)	(-,ID2∗)	(-,ID2∗)	(-,ID2∗)
ID3	(✓,-)	(✓,-)	(✓,-)	(✓,-)	(-,ID3∗)	(-,ID3∗)	(-,ID3∗)	(-,ID3∗)
ID4	(✓,-)	(✓,-)	(✓,-)	(✓,-)	(✓,-)	(-,ID4∗)	(-,ID4∗)	(-,ID4∗)
ID5	(✓,-)	(✓,-)	(✓,-)	(✓,-)	(✓,-)	(✓,-)	(-,ID5∗)	(-,ID5∗)
ID6	(✓,-)	(✓,-)	(✓,-)	(✓,-)	(✓,-)	(✓,-)	(✓,-)	(-,ID6∗)
BM	(✓,-)	(✓,)	(✓,-)	(✓,-)	(✓,-)	(✓,-)	(✓,-)	(-,BM∗)

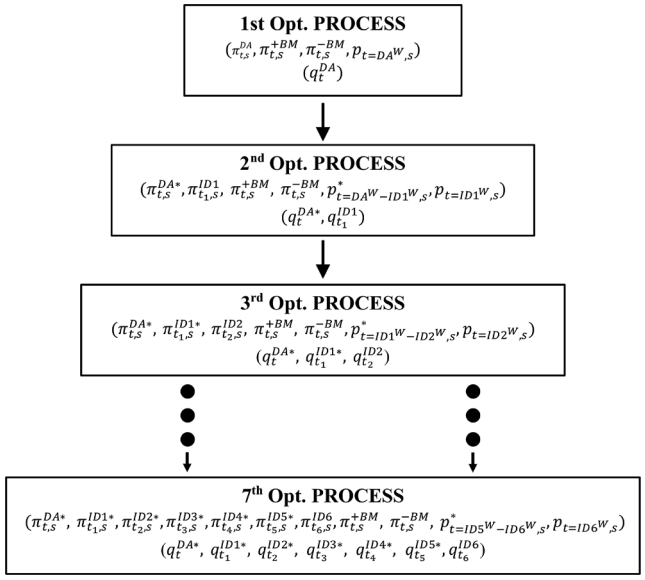

Fig. 1. Optimization processes of SMILP-RSM-1.

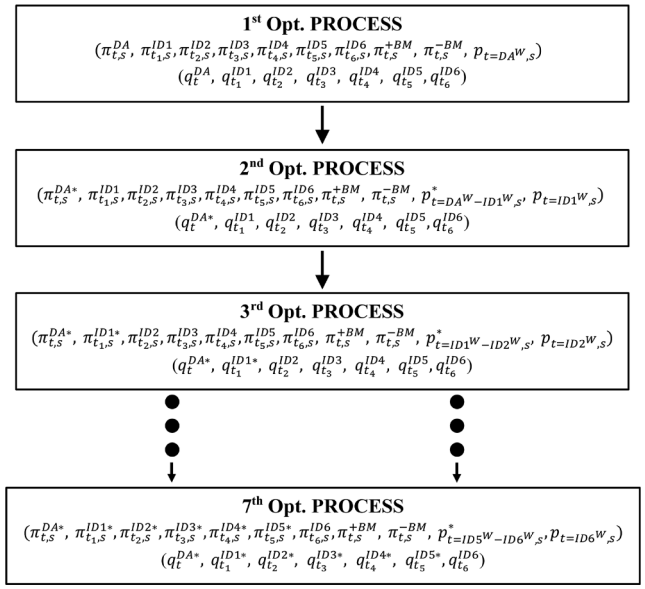

Fig. 2. Optimization processes of SMILP-RSM-2.

brackets). Second, the variables presented in the Figs. 1 and 2 are market bids for each strategy and optimization process (the second row in brackets). Once the key parameters and variables of the optimization process are rendered known, they are propagated to the next optimization process. These parameters are the prices and PV production of the previous market window, as well as bids of previous scheduling or rescheduling. This updated information is relevant because the PV power producer can change the market bid in the actual market window session. The next optimization process will consider the actual parameters of previous market windows as well as previous market bid decisions. For this reason, there is a parameter, namely PV production, which is updated using the hourly difference between the two session windows. For example, $p^*_{t=DA^W-ID1^W}$, $t = DA^W - ID1^W$ represents the hours of the DA windows market that are not shared with the ID1 session window according to Table 2.

Flows of information are sketched in Figs. 3 and 4 for both strategies and each market window. Each strategy has eight optimization processes, and each process has distinct inputs and outputs. The inputs are PV and price forecasts, while the outputs are linked to the next optimization process. The two strategies run the models before the market window starts, and the time horizon of the decisions spans from the opening market window of the process to the end of day D. Once day D has ended, the 8 th optimization process is run with the output of the 7th optimization process that also gathers the outputs of the previous optimization processes.

Finally, CVaR plays an essential role in decision making as it quantifies the risk that the PV producer faces in each optimization process. Decisions depend on risk aversion, which is expressed through $\beta_{i=1,2,3,\ldots,7}$, where i denotes the relevant optimization process.

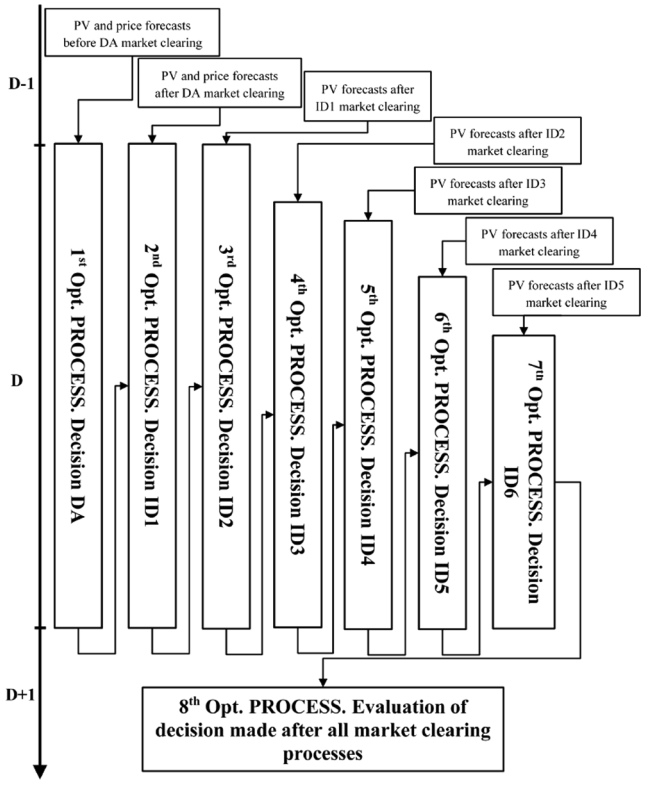

Fig. 3. Information flows SMILP-RSM-1.

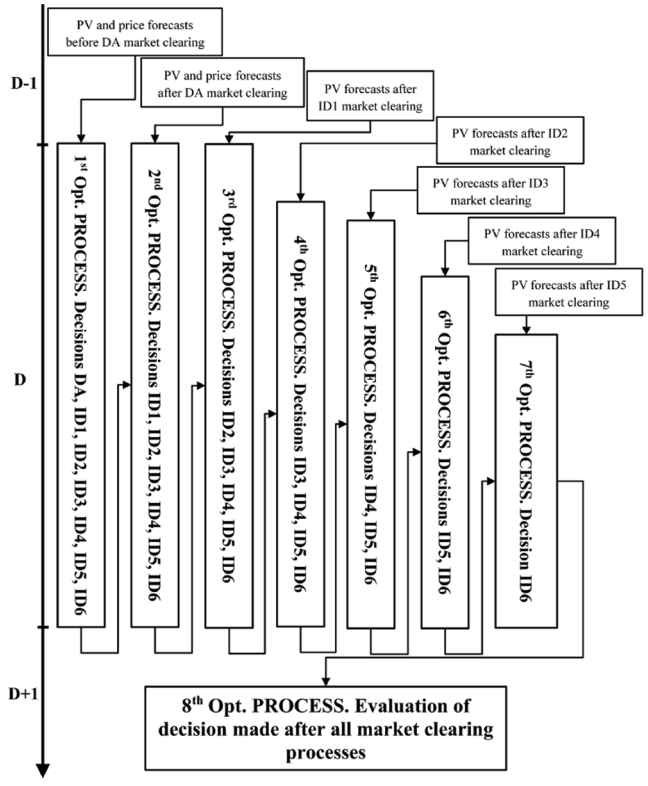

Fig. 4. Information flows in SMILP-RSM-2.

3.1. Set of models 1: SMILP-RSM-1

This strategy focuses only on optimizing decisions in each market floor independently (DA, ID1, ID2, ID3, ID4, ID5, ID6). BM penalizes decisions based on the resulting imbalance. The involved optimization processes use both optimal decisions and real information according to Table 3 and Fig. 1.

3.1.1. First optimization process: DA market scheduling

The first optimization problem results in the DA market decisions that might be penalized by the BM.

Objective function. The objective function (4) maximizes the expected operational profits and CVaR. The expected profit comes from trading the PV production in the DA, penalized through BM. As (4) is essentially a composite objective function that comprises two different objectives, the Pareto frontier is approximated by varying β_1. The main decision for the producer is the quantity to bid in the DA market, $\Phi_1 = \{q_t^{DA}\}$.

$$\text{Maximize}(1-\beta_1)\cdot PF^{PV} + \beta_1 \cdot CVaR. \tag{4}$$

The total expected profit PF^{PV} is the summation of the profit in each period t and scenario s (5). The profit in each period t and scenario s (6) of the PV power producer comes from trading the energy q_t^{DA} in the DA market multiplied by the DA market price $\pi_{t,s}^{DA}$. Once the PV power producer has traded the production in the DA, an imbalance will exist that is penalized through the BM. When the power producer has an upward imbalance $B_{t,s}^{+}$, it is penalized with the upward imbalance market price $\pi_{t,s}^{+BM}$. However, if the PV power producer produces less energy than traded, i.e., has a downward imbalance, it will, in turn, have to pay the downward imbalance $B_{t,s}^{-}$ multiplied by $\pi_{t,s}^{-BM}$. Note that imbalance costs follow the Eqs. (1)–(3). As the PV production and market prices are uncertain, the model decides the volume of energy to submit to the DA market, depending on the risk-hedging attitude of the decision maker.

$$PF^{PV} = \sum_{s\in\mathscr{S}} \rho_s \sum_{t\in\mathscr{T}} PF_{t,s}^{PV}; \tag{5}$$

$$PF_{t,s}^{PV} = \pi_{t,s}^{DA}\cdot q_t^{DA} + \pi_{t,s}^{+BM}\cdot B_{t,s}^{+} - \pi_{t,s}^{-BM}\cdot B_{t,s}^{-};\forall\, t\in\mathscr{T},\ \forall\, s\in\mathscr{S}. \tag{6}$$

The problem constraints are divided into three blocks: risk, market, and imbalance constraints.

Risk constraints. Eqs. (7) and (8) are used to define the CVaR metric. Risk hedging controls the expected value of the tail of the profit distribution with a confidence level $1-\alpha$. When the expected value of the tail of the profit distribution is negative (negative profit is loss), the objective function minimizes the CVaR, while if the expected value of the tail of the profit distribution is positive, the objective function maximizes the CVaR.

$$CVaR = VaR - \frac{1}{1-\alpha}\cdot \sum_{s\in\mathscr{S}} \rho_s\cdot\eta_s; \tag{7}$$

$$-\Big(\sum_{t\in\mathscr{T}} PF_{t,s}^{PV}\Big) + CVaR - \eta_s \leqslant 0\ ;\forall\, s\in\mathscr{S}. \tag{8}$$

Market constraints. Bids have to be non-negative as expressed by (9), while they cannot exceed the installed capacity of the PV power plant as dictated (10).

$$q_t^{DA} \geqslant 0\ ;\forall\, t\in\mathscr{T}; \tag{9}$$

$$q_t^{DA} \leqslant E^{MAX}\ ;\forall\, t\in\mathscr{T}. \tag{10}$$

Imbalance constraints. DA market bids are based on scenarios, i.e., imbalances may occur. Imbalance volumes $B_{t,s}$ are calculated by (11). By definition, these imbalances are calculated as the difference between the actual production $p_{t,s}$ and the DA bid quantity q_t^{DA}. The imbalance volume can be either positive or negative, as it is expressed by (12). This subtraction is possible because of the disjunctive constraints (13) and (14) that involve the binary variable $w_{t,s}$ that determines the direction of the imbalance volume. For modelling purposes, the non-negativity of the positive and negative imbalance volumes is enforced by (15).

$$B_{t,s} = p_{t,s} - q_t^{DA}\ ;\forall\, t\in\mathscr{T},\ \forall\, s\in\mathscr{S}; \tag{11}$$

$$B_{t,s} = B_{t,s}^{+} - B_{t,s}^{-}\ ;\forall\, t\in\mathscr{T},\ \forall\, s\in\mathscr{S}; \tag{12}$$

$$B_{t,s}^{-} \leqslant E^{MAX}\cdot w_{t,s}\ ;\forall\, t\in\mathscr{T},\ \forall\, s\in\mathscr{S}; \tag{13}$$

$$B_{t,s}^{+} \leqslant E^{MAX}\cdot(1-w_{t,s})\ ;\forall\, t\in\mathscr{T},\ \forall\, s\in\mathscr{S}; \tag{14}$$

$$B_{t,s}^{-} \geqslant 0; B_{t,s}^{+} \geqslant 0\ ;\forall\, t\in\mathscr{T},\ \forall\, s\in\mathscr{S}. \tag{15}$$

3.1.2. Second to eighth optimization processes: rescheduling ID1-ID6 and post-market evaluation

Conceptually, optimization processes establish the evaluation of different markets as shown in Table 3. The constraints involved in these markets are similar to those presented in Section 3.1.1 and therefore, for the sake of brevity, only the new variables introduced in each sessions are described in this section.

Once the DA market bid q_t^{DA} has been decided in the 1st optimization process, $\Phi_1 = \{q_t^{DA}\}$, $q_t^{DA^*}$ and the actual DA electricity market prices $\pi_{t,s}^{DA^*}$ are known in the 2nd optimization process. Hence, the bid of ID1 is included in the expected profit and imbalance equations, i.e., (5), (6), and (11), respectively. The bid of ID1 (ID6), $q_{t_1}^{ID1}$ ($q_{t_j}^{IDj}$), can be either a purchase or sale bid for this optimization process, with a positive and negative limit, E^{MAX}. These limits are similar to the rest of the intraday sessions in other optimization processes.

After the first rescheduling, the actual income from the DA market added to the ID1 rescheduling results, $\Phi_2 = \{q_t^{ID1}\}$ is evaluated. SMILP-RSM-1 features seven such optimization processes, while the 8th is used

to calculate the actual profit, with all the information at hand.

3.2. Set of models 2: SMILP-RSM-2

In contrast with the SMILP-RSM-1 strategy, the second set of models proposes to make decisions during each optimization process by jointly considering all markets and intraday sessions. Rescheduling starts after the first optimization process. An overview of this approach is given in Table 4 and Fig. 2.

3.2.1. First optimization process: DA market scheduling

Objective function. The objective function maximizes the expected operational profits (16). The bids in all of the intraday markets are decision variables of the producer in SMILP-RSM-2. These market bids are $\theta_1 = \{q_t^{DA}, q_{t_1}^{ID1}, q_{t_2}^{ID2}, q_{t_3}^{ID3}, q_{t_4}^{ID4}, q_{t_5}^{ID5}, q_{t_6}^{ID6}\}$. In a similar way to (4), CVaR is also optimized.

$$\text{Maximize}(1-\beta_1)\cdot PF^{PV} + \beta_1 \cdot CVaR. \tag{16}$$

The expected profit is defined in a similar way to (5), but the SMILP-RSM-2 strategy also has six intraday sessions. Note that (17) and (18) include prices and bid variables of the six intraday sessions.

$$PF^{PV} = \sum_{s\in\mathscr{S}} \rho_s \sum_{t\in\mathscr{T}} PF_{t,s}^{PV}; \tag{17}$$

$$\begin{aligned} PF_{t,s}^{PV} &= \pi_{t,s}^{DA}\cdot q_t^{DA} + \pi_{t,s}^{+BM}\cdot B_{t,s}^{+} - \pi_{t,s}^{-BM}\cdot B_{t,s}^{-} \\ &+ \pi_{t_1,s}^{ID1}\cdot q_{t_1}^{ID1} + \pi_{t_2,s}^{ID2}\cdot q_{t_2}^{ID2} + \pi_{t_3,s}^{ID3}\cdot q_{t_3}^{ID3} \\ &+ \pi_{t_4,s}^{ID4}\cdot q_{t_4}^{ID4} + \pi_{t_5,s}^{ID5}\cdot q_{t_5}^{ID5} + \pi_{t_6,s}^{ID6}\cdot q_{t_6}^{ID6}; \\ &\forall\, t\in\mathscr{T}\,;\forall\, t_j\in\mathscr{T}_j; j=1,2,3,4,5,6\,;\forall\, s\in\mathscr{S}. \end{aligned} \tag{18}$$

Given the maximization of the expected profit (16), this objective function follows the constraints of the second strategy SMILP-RSM-2.

Risk constraints. Constraints (7) and (8), which define the CVaR metric, are also included in SMILP-RSM-2.

Market constraints. The bids are defined by (19)–(22). The DA market (sale) bid, (19) and (20) are defined in a similar way to (9) and (10). However, the intraday session bids are different in the sense that a purchase bid is also available. As a result, in sessions ID1-ID6, energy can also be bought as it is implied by (21).

$$q_t^{DA} \geqslant 0\,;\forall\, t\in\mathscr{T}; \tag{19}$$

$$q_t^{DA} \leqslant E^{MAX}\,;\forall\, t\in\mathscr{T}; \tag{20}$$

$$q_{t_j}^{IDj} \geqslant -E^{MAX}\,;\forall\, t_j\in\mathscr{T}_j; j=1,2,3,4,5,6; \tag{21}$$

$$q_{t_j}^{IDj} \leqslant E^{MAX}\,;\forall\, t_j\in\mathscr{T}_j; j=1,2,3,4,5,6. \tag{22}$$

Imbalance constraints. The imbalance volume is defined by (23). In SMILP-RSM-2, the imbalance volume is defined as the production in each scenario $p_{t,s}$ minus the sale bid of the DA market and minus all (purchase/sale) bids in each intraday session. It is to be noted that intraday session bids can be either positive or negative; it is either a sale or a purchase bid, respectively. Constraints (24)–(27) are the same as (12)–(15).

$$\begin{aligned} B_{t,s} &= p_{t,s} - q_t^{DA} - q_{t_1}^{ID1} - q_{t_2}^{ID2} - q_{t_3}^{ID3} - q_{t_4}^{ID4} \\ &- q_{t_5}^{ID5} - q_{t_6}^{ID6}\,;\forall\, t\in\mathscr{T}\,;\forall\, t_j\in\mathscr{T}_j; j=1,2,3,4,5,6\,;\forall\, s\in\mathscr{S}; \end{aligned} \tag{23}$$

$$B_{t,s} = B_{t,s}^{+} - B_{t,s}^{-}\,;\forall\, t\in\mathscr{T},\ \forall\, s\in\mathscr{S}; \tag{24}$$

$$B_{t,s}^{-} \leqslant E^{MAX}\cdot w_{t,s}\,;\forall\, t\in\mathscr{T},\ \forall\, s\in\mathscr{S}; \tag{25}$$

$$B_{t,s}^{+} \leqslant E^{MAX}\cdot(1-w_{t,s})\,;\forall\, t\in\mathscr{T},\ \forall\, s\in\mathscr{S}; \tag{26}$$

$$B_{t,s}^{-} \geqslant 0; B_{t,s}^{+} \geqslant 0\,;\forall\, t\in\mathscr{T},\ \forall\, s\in\mathscr{S}. \tag{27}$$

3.2.2. Second to eighth optimization processes: rescheduling ID1-ID6 and post-market evaluation

The optimization processes that determine the rescheduling in SMILP-RSM-2 are similar to those in SMILP-RSM-1. The difference is that each optimization process in SMILP-RSM-2 takes the decisions of all markets and sessions into account.

If there is not a decision variable in θ_i related to the DA market or any of the intraday sessions ($q_t^{DA}, q_{t_1}^{ID1}, q_{t_2}^{ID2}, q_{t_3}^{ID3}, q_{t_4}^{ID4}, q_{t_5}^{ID5}, q_{t_6}^{ID6}$), this means that the decisions in θ_i are known, i.e., they are either optimal values from previous optimization processes or updated information.

4. Case study

4.1. Input data

To test SMILP-RSM-1 and SMILP-RSM2, a PV power producer located in the Navarra region, in the north of Spain, is considered. Historical irradiance data were acquired from the meteorological station of Pamplona (ETSIA) UPNA [48], and were transformed into PV power [MW] using (28), assuming that the PV power producer has a capacity of 50 MW. Then, the maximum PV energy capacity was $E^{MAX} = 50$ MWh. The Spanish day-ahead and intraday market price data were extracted from [4], while imbalance market prices were obtained from [47].

$$P^{PV} = \Big(\sum_{n=1}^{N} \eta_n^{PV}\cdot A_n^{PV}\cdot G\Big)/10^6 \tag{28}$$

In (28) η_n^{PV} (=0.143) is the efficiency of the PV panels in each array, A_n^{PV} (=1.6x12 m^2) is the area of the PV panels in each array, N (=18200) is the number of arrays, and G (W/m^2) is the solar irradiance.

All the market prices and PV production are considered as random variables; for this reason, the model attempts to capture the uncertainty through a finite number of scenarios. The reference day for the simulations is May 1, 2018; Figs. 5 and 6 portray the actual prices and PV production on the reference day, respectively.

4.2. Scenario generation

The scenario trees that were used in this paper are portrayed in Fig. 7.

4.2.1. Day-ahead market prices

To generate scenarios for the DA market prices, the path-based approach that was presented in [49,50] was adapted by replacing the base regression model. The methodology is based on utilizing regression models to obtain one-step-ahead predictions and perturbing their

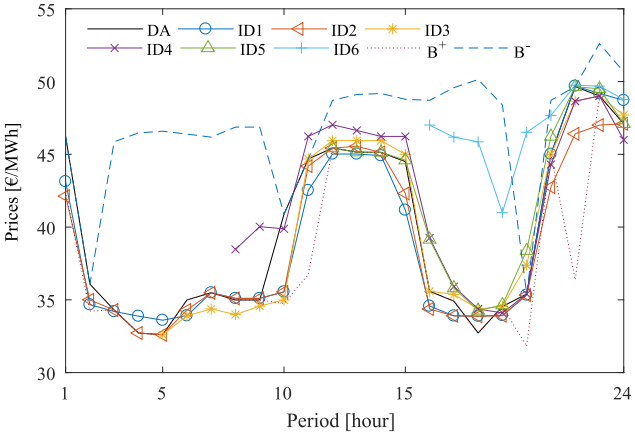

Fig. 5. Actual prices in all the considered market sessions.

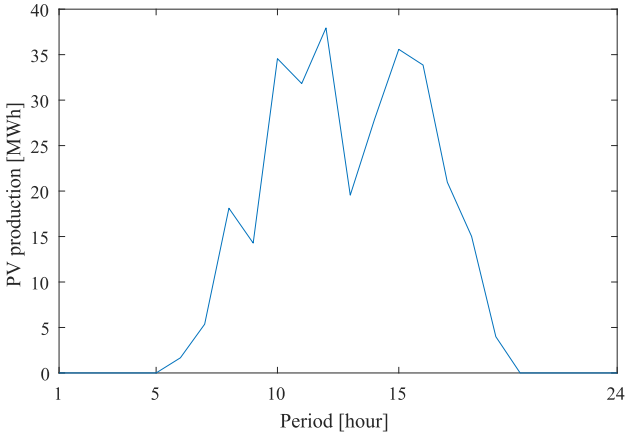

Fig. 6. Actual PV production.

output by sampling Gaussian white noise that is estimated by the residuals during the regression model training phase. Then, the perturbed prediction is used as a predictor in the next one-step prediction, while this process continues until a scenario (path) for the desired lead time has been obtained. By iteratively applying this technique, starting from the first one-step-ahead prediction, the desired number of scenarios can be generated.

The base regression model that was employed in this case is called Ridge regression. To train the regression model and generate scenarios for May 1, 2018, historical data spanning April 25, 2018 to April 30, 2018 were used. Initially, 72 consecutive lags were used as features to perform a one-step-ahead prediction, whereas the number of features was reduced to 24 by performing feature selection using random forest regression [51]. Following the previously described scenario generation procedure, 50 equiprobable DA market price scenarios were generated.

It should be noted that, in contrast with the other random variables considered in the proposed stochastic program formulation, scenarios for the DA market prices only need to be generated once, because after the clearing of the DA market, the actual prices are known.

4.2.2. PV power production

For the generation of irradiance scenarios, the same approach used for the DA market prices was applied. Evidently, PV power production scenarios are obtained by applying (28) on generated irradiance scenarios.

Nonetheless, several adaptations were made to the DA market price scenario generation approach. First, instead of Ridge regression models, Artificial Neural Networks (ANNs) were used to perform one-step ahead predictions. Second, the set of irradiance scenarios was updated before the clearing of the DA market and before each rescheduling following the program of the intraday market to account for the latest information on actual irradiance. As a result, seven sets, comprising 50 scenarios each, were generated in a rolling-shrinking horizon.

To train the ANNs and generate scenarios for May 1, 2018, historical data spanning April 20, 2018 to April 30, 2018, 12:00 PM were used. Initially, 48 consecutive lags were used as features; however, the number of features was reduced to 12 by performing feature selection using random forest regression.

4.2.3. Intraday market prices

As can be seen in Fig. 5, the intraday market prices are strongly correlated with DA market prices. For this reason, a second order polynomial fit was used to estimate the relationship between the DA prices and the prices in each of the intraday sessions based on the historical data (April 20, 2018 to April 30, 2018 12:00 PM). It is to be noted that before the clearing of the DA market, six intraday price signals were generated for each DA market price scenario; however, after the clearing of the DA market, six intraday price signals were generated based on the cleared DA market price.

4.2.4. Imbalance market prices

To generate scenarios for the positive and negative imbalance prices, a different approach was used. Initially, the difference between the DA market price and the positive imbalance prices ($\geqslant 0$), along with the difference between the DA market price and the negative imbalance prices ($\leqslant 0$), were obtained for the period between January 1, 2018 and April 30, 2018, 12:00 PM and a non-parametric kernel density estimator was fitted to each difference time series. Subsequently, before the clearing of the DA market, two sets of 24 samples (one for each price difference and period) were drawn from the non-parametric distribution and were superposed to the 50 DA market price scenarios. After the clearing of the DA market, the samples of the differences were used to adjust the estimation of the positive and negative imbalance market prices based on the subsequently known DA market prices.

4.3. Results and discussion

After having run the simulations, the PV power producer's behavior follows the scenario profiles of PV production and market prices. The bidding profiles in the DA market and the ID market sessions both depend on the scenarios trees but also on the particular trading strategy. The bids in all the markets under both SMILP-RSM-1 and SMILP-RSM-2 strategies are shown in Tables 5–10.

The results of each of the seven optimization processes that are

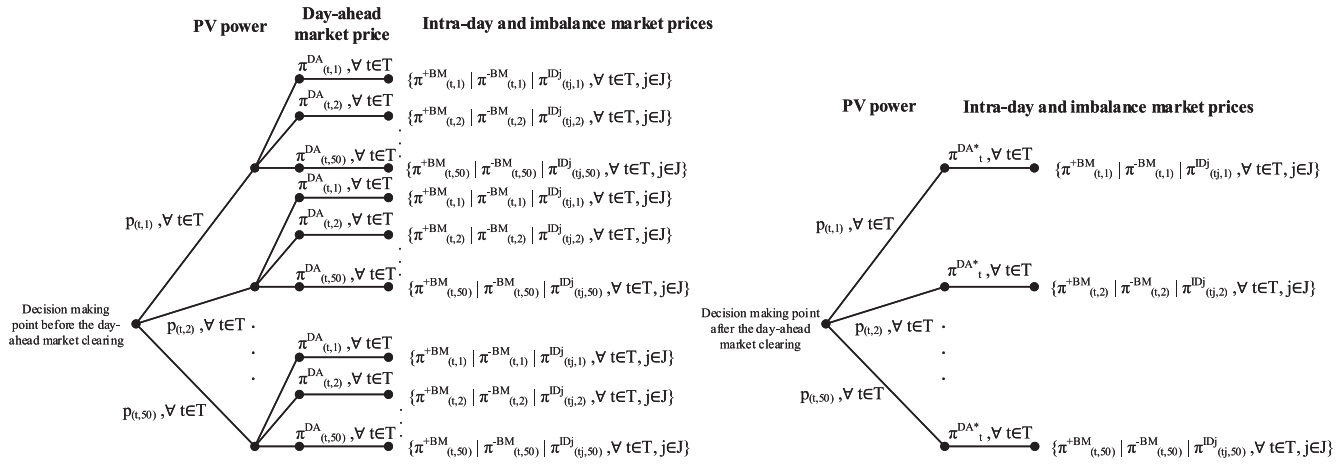

Fig. 7. Scenario tree before and after the DA market clearing. The scenario tree on the right is updated by incorporating newly available information before performing rescheduling, according to the program of the intraday market.

Table 5
Results of the bids (MWh) for the SMILP-RSM-1 in each hour and market sessions for $\beta_{i=1,2,3,\ldots,7} = 0.9$, and from the 1st to the 7th optimization processes.

Hour	DA	ID1	ID2	ID3	ID4	ID5	ID6
1	0,0	0,0	0,0	0,0	0,0	0,0	0,0
2	0,0	0,0	0,0	0,0	0,0	0,0	0,0
3	0,0	0,0	0,0	0,0	0,0	0,0	0,0
4	0,0	0,0	0,0	0,0	0,0	0,0	0,0
5	0,0	0,0	0,0	0,0	0,0	0,0	0,0
6	1,6	48,4	0,0	0,0	0,0	0,0	0,0
7	0,2	−0,2	0,8	1,8	0,0	0,0	0,0
8	2,5	2,0	1,4	46,8	−1,8	0,0	0,0
9	21,1	32,8	1,5	−2,3	0,6	0,0	0,0
10	31,7	27,6	0,9	−5,6	−41,7	0,0	0,0
11	28,0	35,7	−0,1	−42,0	−34,8	0,0	0,0
12	19,1	−0,9	−1,9	−27,5	3,6	35,2	0,0
13	15,9	−2,8	−1,5	−26,8	0,3	50,0	0,0
14	9,2	−6,6	−1,4	−23,7	23,0	−29,1	0,0
15	27,5	25,1	2,8	−50,0	44,7	−50,0	0,0
16	22,0	29,6	0,1	−1,7	0,0	−50,0	−46,8
17	4,4	46,0	0,3	−0,7	0,0	−50,0	−50,0
18	9,5	40,5	0,0	0,0	−50,0	−48,9	−9,8
19	0,0	1,9	−1,9	50,0	−50,0	−50,0	−12,9
20	0,0	0,0	0,0	0,0	0,0	0,0	0,0
21	0,0	0,0	0,0	0,0	0,0	0,0	0,0
22	0,0	0,0	0,0	0,0	0,0	0,0	0,0
23	0,0	0,0	0,0	0,0	0,0	0,0	0,0
24	0,0	0,0	0,0	0,0	0,0	0,0	0,0

Table 6
Results of the bids (MWh) for the SMILP-RSM-2 in each hour and market sessions for $\beta_{i=1} = 0.9$, and the 1st optimization process.

Hour	DA	ID1	ID2	ID3	ID4	ID5	ID6
1	0,0	0,0	0,0	0,0	0,0	0,0	0,0
2	0,0	0,0	0,0	0,0	0,0	0,0	0,0
3	0,0	0,0	0,0	0,0	0,0	0,0	0,0
4	0,0	0,0	0,0	0,0	0,0	0,0	0,0
5	0,0	0,0	0,0	0,0	0,0	0,0	0,0
6	0,0	−50,0	50,0	50,0	0,0	0,0	0,0
7	0,0	−50,0	0,7	50,0	0,0	0,0	0,0
8	0,0	−50,0	−47,5	50,0	50,0	0,0	0,0
9	50,0	−50,0	−50,0	50,0	16,4	0,0	0,0
10	50,0	−50,0	25,1	50,0	−50,0	0,0	0,0
11	0,0	50,0	50,0	−26,3	−50,0	0,0	0,0
12	44,3	50,0	−27,6	−50,0	−50,0	50,0	0,0
13	39,9	−24,0	50,0	−50,0	−50,0	50,0	0,0
14	0,0	50,0	50,0	−50,0	13,2	−50,0	0,0
15	0,0	50,0	50,0	−50,0	50,0	−50,0	0,0
16	0,0	50,0	50,0	3,2	50,0	−50,0	−50,0
17	0,0	0,6	50,0	50,0	50,0	−50,0	−50,0
18	7,6	50,0	50,0	50,0	−50,0	−50,0	−50,0
19	0,0	50,0	50,0	50,0	−50,0	−50,0	−50,0
20	0,0	0,0	0,0	0,0	0,0	0,0	0,0
21	0,0	0,0	0,0	0,0	0,0	0,0	0,0
22	0,0	0,0	0,0	0,0	0,0	0,0	0,0
23	0,0	0,0	0,0	0,0	0,0	0,0	0,0
24	0,0	0,0	0,0	0,0	0,0	0,0	0,0

Table 7
Results of the bids (MWh) for the SMILP-RSM-2 in each hour and market sessions for $\beta_{i=2} = 0.9$, and the 2nd optimization process.

Hour	DA	ID1	ID2	ID3	ID4	ID5	ID6
1	0,0	0,0	0,0	0,0	0,0	0,0	0,0
2	0,0	0,0	0,0	0,0	0,0	0,0	0,0
3	0,0	0,0	0,0	0,0	0,0	0,0	0,0
4	0,0	0,0	0,0	0,0	0,0	0,0	0,0
5	0,0	0,0	0,0	0,0	0,0	0,0	0,0
6	0,0	−50,0	50,0	50,0	0,0	0,0	0,0
7	0,0	−50,0	0,0	50,0	0,0	0,0	0,0
8	0,0	−50,0	−45,4	50,0	50,0	0,0	0,0
9	50,0	−50,0	−46,1	50,0	50,0	0,0	0,0
10	50,0	−40,7	50,0	50,0	−50,0	0,0	0,0
11	0,0	50,0	50,0	−30,5	−50,0	0,0	0,0
12	44,3	50,0	−26,0	−50,0	−50,0	50,0	0,0
13	39,9	−26,8	50,0	−50,0	−50,0	50,0	0,0
14	0,0	50,0	50,0	−50,0	2,6	−50,0	0,0
15	0,0	50,0	50,0	−50,0	50,0	−50,0	0,0
16	0,0	50,0	50,0	1,6	50,0	−50,0	−50,0
17	0,0	0,4	50,0	50,0	50,0	−50,0	−50,0
18	7,6	50,0	50,0	50,0	−50,0	−50,0	−50,0
19	0,0	50,0	50,0	50,0	−50,0	−50,0	−50,0
20	0,0	0,0	0,0	0,0	0,0	0,0	0,0
21	0,0	0,0	0,0	0,0	0,0	0,0	0,0
22	0,0	0,0	0,0	0,0	0,0	0,0	0,0
23	0,0	0,0	0,0	0,0	0,0	0,0	0,0
24	0,0	0,0	0,0	0,0	0,0	0,0	0,0

Table 8
Results of the bids (MWh) for the SMILP-RSM-2 in each hour and market sessions for $\beta_{i=3} = 0.9$, and the 3rd optimization process.

Hour	DA	ID1	ID2	ID3	ID4	ID5	ID6
1	0,0	0,0	0,0	0,0	0,0	0,0	0,0
2	0,0	0,0	0,0	0,0	0,0	0,0	0,0
3	0,0	0,0	0,0	0,0	0,0	0,0	0,0
4	0,0	0,0	0,0	0,0	0,0	0,0	0,0
5	0,0	0,0	0,0	0,0	0,0	0,0	0,0
6	0,0	−50,0	50,0	50,0	0,0	0,0	0,0
7	0,0	−50,0	0,7	50,0	0,0	0,0	0,0
8	0,0	−50,0	−44,0	50,0	50,0	0,0	0,0
9	50,0	−50,0	−44,6	50,0	50,0	0,0	0,0
10	50,0	−40,7	50,0	50,0	−50,0	0,0	0,0
11	0,0	50,0	50,0	−28,8	−50,0	0,0	0,0
12	44,3	50,0	−28,0	−50,0	−50,0	50,0	0,0
13	39,9	−26,8	48,5	−50,0	−50,0	50,0	0,0
14	0,0	50,0	50,0	−50,0	1,2	−50,0	0,0
15	0,0	50,0	50,0	−50,0	50,0	−50,0	0,0
16	0,0	50,0	50,0	1,7	50,0	−50,0	−50,0
17	0,0	0,4	50,0	50,0	50,0	−50,0	−50,0
18	7,6	50,0	50,0	50,0	−50,0	−50,0	−50,0
19	0,0	50,0	50,0	50,0	−50,0	−50,0	−50,0
20	0,0	0,0	0,0	0,0	0,0	0,0	0,0
21	0,0	0,0	0,0	0,0	0,0	0,0	0,0
22	0,0	0,0	0,0	0,0	0,0	0,0	0,0
23	0,0	0,0	0,0	0,0	0,0	0,0	0,0
24	0,0	0,0	0,0	0,0	0,0	0,0	0,0

executed under SMILP-RSM-1 are displayed in each column of Table 5. The behavior of the bid depends on the scenarios of prices and PV production for the window of the scheduling or rescheduling, which is taking the decisions. Although the imbalances also affect the bids, these imbalances can come from previous scheduling or rescheduling.

Following the optimization processes of the SMILP-RSM-2 strategy in Table 4, it can be seen that the 5th and 6th processes have the same results as the 7th optimization process as shown in Table 10. For this reason, it is important to take note when each optimization process moves forward. The next optimization process has fewer decisions because the previous scheduling or rescheduling is now known. So some positions in the bid come from taking advantages of the arbitrage between market and sessions. Similar results in the 5-6th optimization processes happen as a consequence of lower uncertainty and length of horizon considered in the rescheduling process.

As we can observe in Tables 5–10, owing to different session windows, there is a reduction of traded hours in the last rescheduling. This reduction means that the bids in DA column span from the 6th to the 18th hours, while the ID6 column has only 4 h of bids, from the 16th to the 19th hour. Also, between the 1st and the 5th hours and from the 20th to the 24th hours, the bid is zero due to the sunrise and sunset times in that period of the year.

SMILP-RSM-2 presents higher bid volumes compared to SMILP-RSM-1. SMILP-RSM-1 considers only one market and penalties through the balancing market. Then, model SMILP-RSM-1 compensates the

Table 9
Results of the bids (MWh) for the SMILP-RSM-2 in each hour and market sessions for $\beta_{i=4} = 0.9$, and the 4th optimization process.

Hour	DA	ID1	ID2	ID3	ID4	ID5	ID6
1	0,0	0,0	0,0	0,0	0,0	0,0	0,0
2	0,0	0,0	0,0	0,0	0,0	0,0	0,0
3	0,0	0,0	0,0	0,0	0,0	0,0	0,0
4	0,0	0,0	0,0	0,0	0,0	0,0	0,0
5	0,0	0,0	0,0	0,0	0,0	0,0	0,0
6	0,0	−50,0	50,0	50,0	0,0	0,0	0,0
7	0,0	−50,0	0,7	50,0	0,0	0,0	0,0
8	0,0	−50,0	−44,0	50,0	50,0	0,0	0,0
9	50,0	−50,0	−44,6	50,0	47,7	0,0	0,0
10	50,0	−40,7	50,0	45,2	−50,0	0,0	0,0
11	0,0	50,0	50,0	−28,5	−50,0	0,0	0,0
12	44,3	50,0	−28,0	−50,0	−50,0	50,0	0,0
13	39,9	−26,8	48,5	−50,0	−50,0	50,0	0,0
14	0,0	50,0	50,0	−50,0	0,7	−50,0	0,0
15	0,0	50,0	50,0	−50,0	50,0	−50,0	0,0
16	0,0	50,0	50,0	0,0	50,0	−50,0	−50,0
17	0,0	0,4	50,0	49,6	50,0	−50,0	−50,0
18	7,6	50,0	50,0	50,0	−50,0	−50,0	−50,0
19	0,0	50,0	50,0	50,0	−50,0	−50,0	−50,0
20	0,0	0,0	0,0	0,0	0,0	0,0	0,0
21	0,0	0,0	0,0	0,0	0,0	0,0	0,0
22	0,0	0,0	0,0	0,0	0,0	0,0	0,0
23	0,0	0,0	0,0	0,0	0,0	0,0	0,0
24	0,0	0,0	0,0	0,0	0,0	0,0	0,0

Table 10
Results of the bids (MWh) for the SMILP-RSM-2 in each hour and market sessions for $\beta_{i=7} = 0.9$, and the 7th optimization process.

Hour	DA	ID1	ID2	ID3	ID4	ID5	ID6
1	0,0	0,0	0,0	0,0	0,0	0,0	0,0
2	0,0	0,0	0,0	0,0	0,0	0,0	0,0
3	0,0	0,0	0,0	0,0	0,0	0,0	0,0
4	0,0	0,0	0,0	0,0	0,0	0,0	0,0
5	0,0	0,0	0,0	0,0	0,0	0,0	0,0
6	0,0	−50,0	50,0	50,0	0,0	0,0	0,0
7	0,0	−50,0	0,7	50,0	0,0	0,0	0,0
8	0,0	−50,0	−44,0	50,0	50,0	0,0	0,0
9	50,0	−50,0	−44,6	50,0	48,4	0,0	0,0
10	50,0	−40,7	50,0	45,2	−50,0	0,0	0,0
11	0,0	50,0	50,0	−28,5	−50,0	0,0	0,0
12	44,3	50,0	−28,0	−50,0	−50,0	50,0	0,0
13	39,9	−26,8	48,5	−50,0	−50,0	50,0	0,0
14	0,0	50,0	50,0	−50,0	0,5	−50,0	0,0
15	0,0	50,0	50,0	−50,0	50,0	−50,0	0,0
16	0,0	50,0	50,0	0,0	50,0	−50,0	−50,0
17	0,0	0,4	50,0	49,6	50,0	−50,0	−50,0
18	7,6	50,0	50,0	50,0	−50,0	−50,0	−50,0
19	0,0	50,0	50,0	50,0	−50,0	−50,0	−50,0
20	0,0	0,0	0,0	0,0	0,0	0,0	0,0
21	0,0	0,0	0,0	0,0	0,0	0,0	0,0
22	0,0	0,0	0,0	0,0	0,0	0,0	0,0
23	0,0	0,0	0,0	0,0	0,0	0,0	0,0
24	0,0	0,0	0,0	0,0	0,0	0,0	0,0

imbalances later in other rescheduling processes. Nevertheless, SMILP-RSM-2 includes all forward markets in each scheduling and rescheduling process. SMILP-RSM-2 can then buy or sell more energy in subsequent rescheduling processes because it considers all markets, which means that penalties can be further mitigated. Nonetheless, it should be noted that SMILP-RSM-2 could lead to more losses owing to the exhibited arbitrage behavior. The mitigation of penalties also comes from reducing the uncertainty because of the reducing rescheduling horizons.

A post-market analysis allows the calculation of the actual profit, CVaR, and the imbalances following each strategy and for each risk-aversion level β_i. The actual profits and imbalances for both strategies and for $\beta_{i=1,2,3,\ldots,7} = 0{,}1$ and $\beta_{i=1,2,3,\ldots,7} = 0{,}9$ are displayed in Table 11. It can be observed that the highest negative imbalances occur under all strategies and for all values of β in hour 6. Owing to the high negative imbalance, the real profit is negative during that period. However, the negative imbalance is not the unique factor that affects profit. Profit depends on the differences between DA and ID prices, the imbalance prices, and PV production. Their effects on the profits also depend on scenarios and on how well these are able to describe the future. For the mitigation of unknown future effects on trading, different markets and sessions are used. For this reason, the scheduling and rescheduling present different expected profits. Also, it should be noted that the expected profits of SMILP-RSM-2 are higher than that of SMILP-RSM-1.

Negative imbalances under SMILP-RSM-1 are the same for both β_i, while the positive imbalances are higher when β_i is higher. These higher positive imbalances mean that the bids in markets are lower than the production; the income of the producer from the market is then also lower. In other words, the lowest real profit happens when the upward imbalance is the highest at $\beta_i = 0.9$ under SMILP-RSM-1. As explained regarding the imbalance penalization, the downward imbalances reduce the profits, but SMILP-RSM-2 has higher actual profits despite the higher negative imbalances in comparison to SMILP-RSM-1. In fact, the negative imbalances happen if the bids are proven higher than the actual production. As can be seen in Table 11, this is the case in SMILP-RSM-2 in comparison with SMILP-RSM-1. In contrast, the upward imbalances are lower in SMILP-RSM-2. The second strategy utilizes arbitrage, an effect of deciding bids in all markets jointly on each optimization process with updated information. This arbitrage comes from the market prices during each optimization process. Each optimization process attempts to take advantage of the differences between future market prices. It can be observed that the actual profits increase by more than 2000 € in the 8th hour when comparing SMILP-RSM-2 with SMILP-RSM-1. This increase is owing to the reduction in the positive imbalance of more than 70 MW.

Figs. 8 (ai) and 9 (ai) portray the profits and CVaR in all the simulations of all optimization processes. These figures also include the different configurations regarding the β_i. Consider each β_i as an independent simulation. For instance, there are five $\beta_{i=1} =$ 0.1, 0.25, 0.5, 0.75, and 0.9 in the 1st optimization process. Later, there are two $\beta_{i=2,3,4,\ldots,7} =$ 0.1, and 0.9 for the other optimization processes. Rescheduling only has two values of β because rescheduling is less sensitive to its value. For this reason we use extreme β values, such as 0.1 and 0.9. As a result, in total, there are 7 optimization processes; the first process has 5 cases, and from the second process to the seventh process, each has an optimization process of 2 cases. In conclusion, the total number of simulations are $5 \times 2 \times 2 \times 2 \times 2 \times 2 \times 2 = 320$ cases with different configurations of β_i.

In addition to the behavior of profits (PF) vs. CVaR for both strategies and with all the β values, Figs. 8 and 9 show a zoom of some PF vs. CVaR areas of interest. SMILP-RSM-1 starts the optimization process with low expected profits. Later, the three following optimization processes reduce the expected profits further as shown in Fig. 8. This reduction can come from real updated DA bids for that market window. The rest of the optimization processes increase the expected profits, for which the final process (post-market), from real profit evaluation, is the highest. Therefore, the last three intraday sessions have more expected profits for all Pareto frontiers. Independently of β, each optimization process has a Pareto frontier in a small area. The Pareto frontier of the first optimization process is a typical frontier of PF vs. CVaR as [25]. It can be observed that, for all the values of the β per optimization

Table 11
Actual profits (€) and imbalances (MWh) of SMILP-RSM-1 (1) and SMILP-RSM-2 (2) for $\beta_{i=1,2,3,\ldots,7} = 0{,}1$ and 0,9.

Str., β **Hour**	**1,** $\beta_i = 0{,}1$ **PF**	**1,** $\beta_i = 0{,}9$ **PF**	**2,** $\beta_i = 0{,}1$ **PF**	**2,** $\beta_i = 0{,}9$ **PF**	**1,** $\beta_i = 0{,}1$ **(**B^+, B^-**)**	**1,** $\beta_i = 0{,}9$ **(**B^+, B^-**)**	**2,** $\beta_i = 0{,}1$ **(**B^+, B^-**)**	**2,** $\beta_i = 0{,}9$ **(**B^+, B^-**)**
1	0,0	0,0	0,0	0,0	0,0	0,0	0,0	0,0
2	0,0	0,0	0,0	0,0	0,0	0,0	0,0	0,0
3	0,0	0,0	0,0	0,0	0,0	0,0	0,0	0,0
4	0,0	0,0	0,0	0,0	0,0	0,0	0,0	0,0
5	0,0	0,0	0,0	0,0	0,0	0,0	0,0	0,0
6	−543,4	−545,1	−473,3	−473,3	−48,3	−48,3	−48,3	−48,3
7	207,5	206,7	649,7	649,7	2,8	2,8	4,7	4,6
8	711,4	736,1	1.732,8	1.732,9	−32,8	−32,8	9,9	12,1
9	12,2	12,5	774,0	774,0	−39,5	−39,5	−39,5	−39,5
10	1.332,5	1.306,6	1.840,4	1.840,4	21,7	21,7	−20,0	−20,0
11	1.472,4	1.331,8	1.788,9	1.713,8	45,1	45,1	−18,2	10,3
12	2.165,7	2.097,3	2.965,0	2.965,0	5,4	10,4	16,8	21,6
13	1.252,7	1.177,7	1.980,8	1.979,6	−15,6	−15,6	1,2	7,9
14	3.094,1	2.806,5	4.037,8	4.041,4	56,5	56,5	23,1	27,4
15	4.408,2	4.402,2	4.176,2	4.176,2	35,6	35,6	−14,4	−14,4
16	4.619,2	4.617,0	5.111,2	5.111,2	80,7	80,7	−16,1	−16,1
17	4.172,3	4.169,7	4.801,5	4.801,5	71,0	71,0	−29,0	−29,0
18	4.091,3	4.096,7	6.311,3	6.311,3	73,8	73,8	0,9	7,4
19	4.733,9	4.762,2	5.980,2	5.980,2	66,9	66,9	4,0	4,0
20	0,0	0,0	0,0	0,0	0,0	0,0	0,0	0,0
21	0,0	0,0	0,0	0,0	0,0	0,0	0,0	0,0
22	0,0	0,0	0,0	0,0	0,0	0,0	0,0	0,0
23	0,0	0,0	0,0	0,0	0,0	0,0	0,0	0,0
24	0,0	0,0	0,0	0,0	0,0	0,0	0,0	0,0
Total	31.730,1	31.177,7	41.676,5	41.603,9	(459,4, −136,2)	(464,4, −136,2)	(60,5, −185,6)	(95,4, −167,4)

process, this follows a linear relation of PF vs. CVaR. This linear relation effect can be attributed to using only two β values in which the profits are in a narrow area.

SMILP-RSM-2 has a different behavior to SMILP-RSM-1, as seen in Fig. 9. SMILP-RSM-2 has the first optimization process as the highest expected profits. Once the 2nd optimization process re-checked the optimal DA bids, the expected profit of the 2nd optimization process is lower. This effect of reducing the expected profits in the 2nd optimization process is a little mitigated in the 3rd optimization process. The next optimization process decreases the expected profit again. After the 4th optimization process, the expected profits increase as well as the CVaR. On the contrary, the real profit (8th process in Fig. 9 is almost the same as the 7th optimization process, but the CVaR is higher.

Comparing Figs. 8 and 9, we observe that SMILP-RSM-1 has a higher range of PF vs. CVaR, from 500 € to 32000 € for the profits. This range is a clear effect of deciding only a market bid ahead in each optimization process. The real profits are lower because SMILP-RSM-1 only considers income from the electricity market. On the contrary, the SMIL-RSM-2 has a range equal to [37000, 43000] €. The narrow range in SMILP-RSM-2 is because each optimization process considers all market bids in advance. From the results of both strategies, we can observe that the speculative offer, SMILP-RSM-2, has better results. This speculation plays with the arbitrage and rescheduling after finishing the previous market window. Despite being a speculative strategy, SMILP-RSM-2 cannot directly influence market prices owing to a low PV capacity compared with the total generation capacity in the power system.

The risk-hedging map allows us to see the behaviour of profits with the risk aversion in two different trading strategies. For both strategies, Figs. 8 and 9 display the risk map. As a result, the first optimization process in both strategies has a similar efficient frontier to [25]. On the contrary, there is another novel optimization processes with a particular risk map. Zooms in Figs. 8 and 9 from the 2nd to the 7th optimization process indicate that its Pareto frontiers are in a very small area. For the first strategy, SMILP-RSM-1, the PF vs. CVaR demonstrates linear behaviour; while the second strategy, SMILP-RSM-2, has a higher dispersion of each PF vs. CVaR evaluation. In addition, the β_i tree for the evaluation of PF vs. CVaR, has unexpected results. This means, each β_i analysis of PF vs. CVaR comes from a previous β_{i-1}, $i \neq 1$. For example, an extreme case is the lowest β_i as $\beta_{i=1} = 0, 1 \rightarrow \beta_{i=2} = 0, 1 \rightarrow \beta_{i=3} = 0, 1 \rightarrow \beta_{i=4} = 0, 1 \rightarrow \beta_{i=5} = 0, 1 \rightarrow \beta_{i=6} = 0, 1 \rightarrow \beta_{i=7} = 0, 1$, which provides the highest profits. From previous optimization processes and β, we could think that profits should follow the previous profit efficient frontier of $\beta_{i=i-1}$, but Figs. 8 and 9 show that each optimization process has its own PF vs. CVaR area in the results of both strategies. For this reason, the optimization process for each session is completely independent.

Finally, Table 12 presents a ratio of the real profit divided by real PV production. This table shows the ratios of the extreme results of the real profits through β_i. The range of results is [103,72, 138,64] €/MWh for the reference day simulated. This range can help with decisions and comparison with feed-in tariffs and power purchase agreements (PPAs).

5. Conclusions

In this paper, two strategies were proposed for trading the energy of a PV power producer in the day-ahead and all sessions of the intraday market, with a final penalization through the balancing market. The mathematical models were based on two-stage stochastic programming. The Conditional Value-at-Risk (CVaR) metric was used to perform risk hedging. Scheduling scenarios were also developed for both the irradiance and wholesale electricity market prices, while the rescheduling scenarios were made following a rolling-shrinking horizon. As a result of the post-market analysis, the distances of the expected and real profits between optimization processes and post-market (8th optimization process) demonstrate how the optimization model behaves.

Based on extensive simulations, the most important conclusions can be summarized as follows:

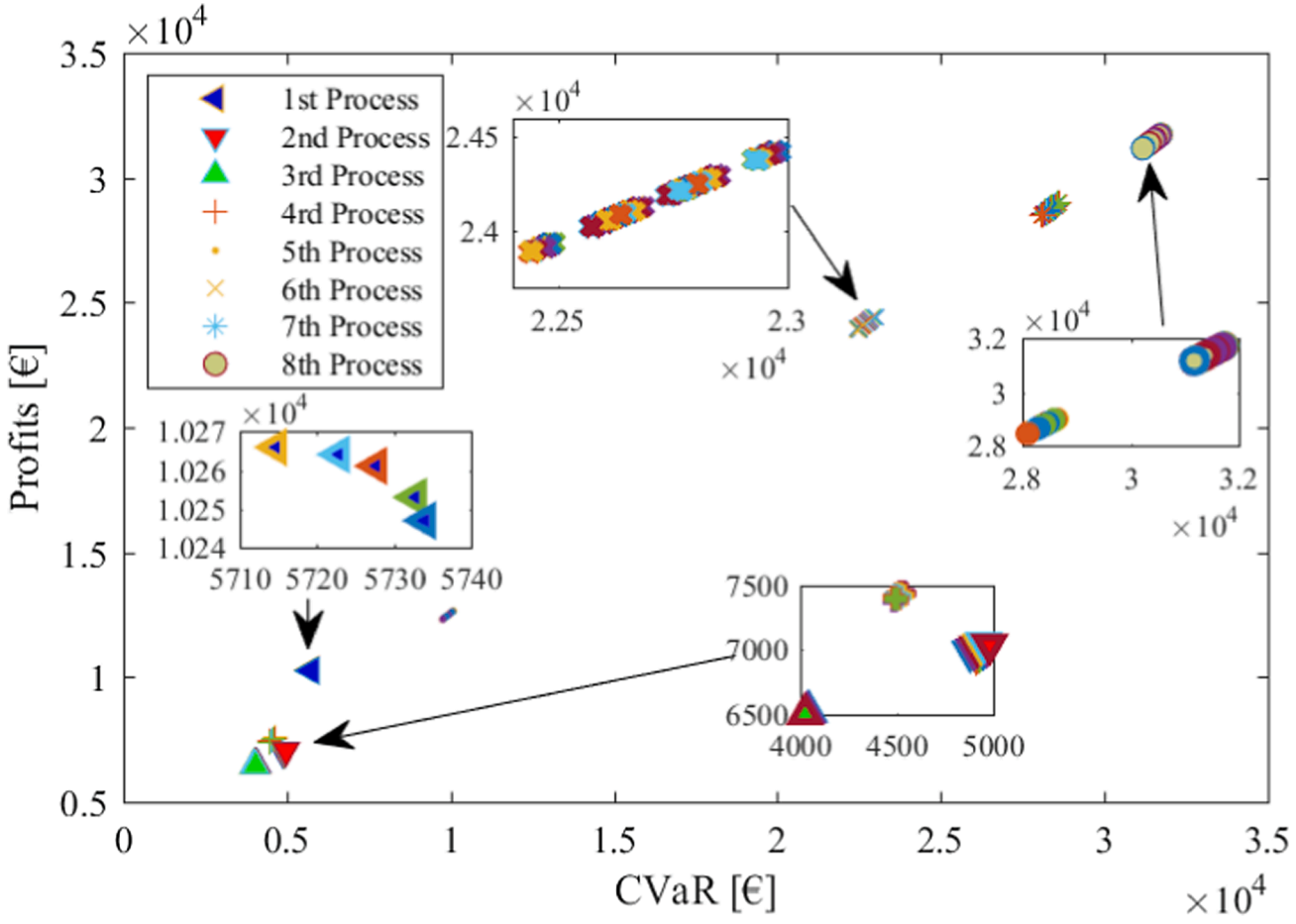

(a) Profit vs. CVaR of SMILP-RSM-1.

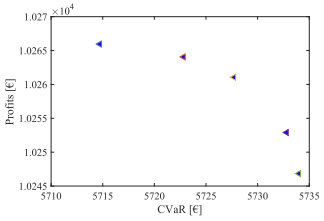

(b) 1st Opt. process.

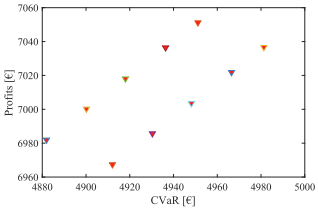

(c) 2nd Opt. process.

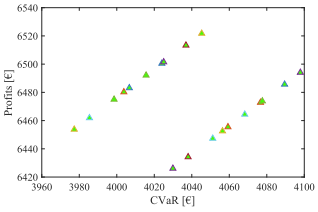

(d) 3rd Opt. process.

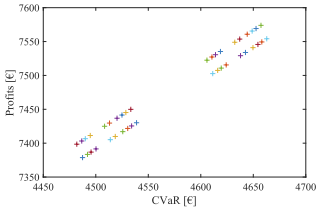

(e) 4th Opt. process.

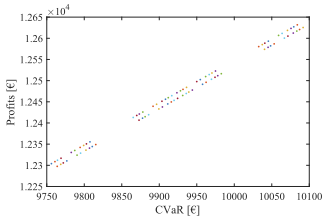

(f) 5th Opt. process.

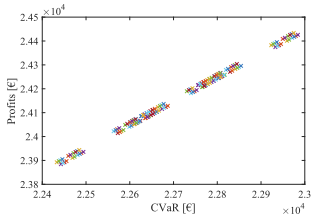

(g) 6th Opt. process.

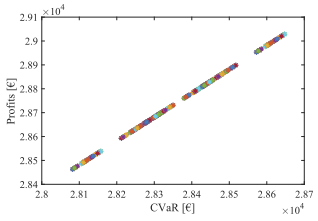

(h) 7th Opt. process.

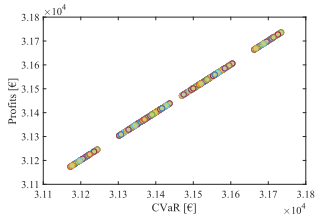

(i) 8th Opt. process.

Fig. 8. Profit vs. CVaR of SMILP-RSM-1.

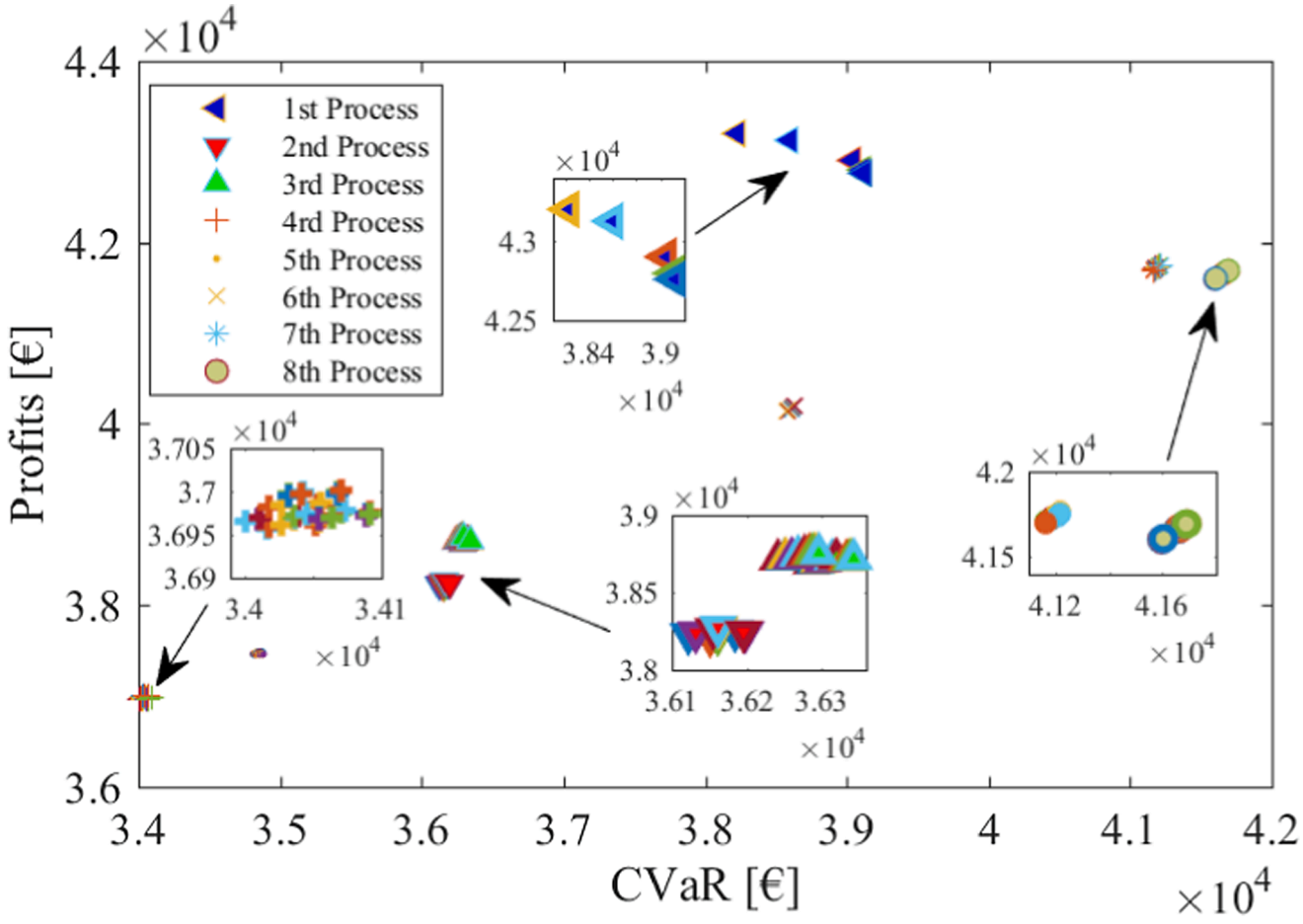

(a) Profit vs. CVaR of SMILP-RSM-2.

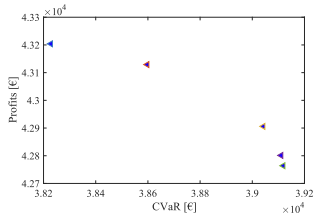

(b) 1st Opt. process.

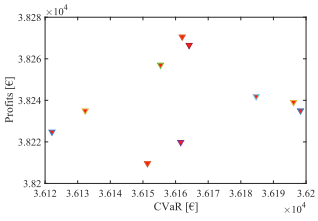

(c) 2nd Opt. process.

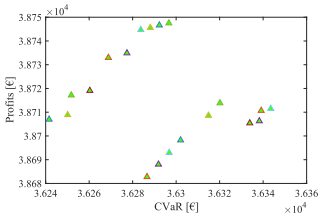

(d) 3rd Opt. process.

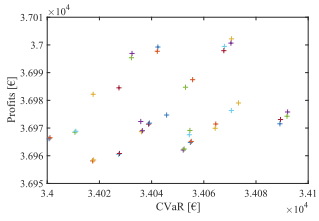

(e) 4th Opt. process.

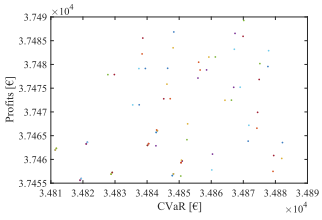

(f) 5th Opt. process.

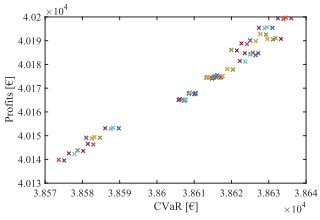

(g) 6th Opt. process.

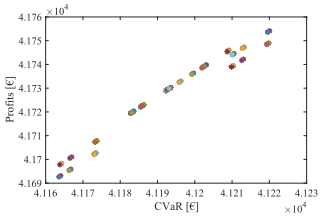

(h) 7th Opt. process.

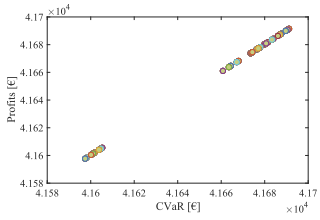

(i) 8th Opt. process.

Fig. 9. Profit vs. CVaR of SMILP-RSM-2.

Table 12
Real PV production (RPV) (MWh), the highest real profit of SMILP-RSM-1 per MWh (RHPF1) (€/MWh), the lowest real profit of SMILP-RSM-1 per MWh (RLPF1) (€/MWh), the highest real profit of SMILP-RSM-2 per MWh (RHPF2) (€/MWh), and the lowest real profit of SMILP-RSM-2 per MWh (RLPF2) (€/MWh).

RPV	RHPF1	RLPF1	RHPF2	RLPF2
300,59	105,55	103,72	138,64	138,40

- SMILP-RSM-2 has the potential to return greater actual profits and more favorable CVaR values than SMILP-RSM-1.
- Speculation and arbitrage in SMILP-RSM-2 reduce the total number of imbalances. The imbalances are reduced owing to a higher amount of energy that is traded throughout different market floors.
- The Pareto frontiers of the expected profit versus CVaR change depending on the current optimization process; however, it is notable that they are not close to the frontier that is produced during the 1st optimization process. The risk-hedging map of expected profit versus CVaR shows that each optimization process results in frontiers that are relatively narrow.
- SMILP-RSM-2 compensates for imbalance penalties with the price differences between market floors, resulting from considering subsequent market floors in day-ahead decisions.

CRediT authorship contribution statement

Agustín A. Sánchez de la Nieta: Conceptualization, Formal analysis, Investigation, Methodology, Software, Writing - original draft, Writing - review & editing. **Nikolaos G. Paterakis:** Conceptualization, Formal analysis, Methodology, Software, Writing - original draft, Writing - review & editing. **Madeleine Gibescu:** Writing - review & editing.

Declaration of Competing Interest

The authors declare that they have no known competing financial interests or personal relationships that could have appeared to influence the work reported in this paper.

Acknowledgement

This project has received funding in the framework of the joint program initiative ERA-Net Smart Grids Plus. The initiative has received funding from the European Unions Horizon 2020 Research and Innovation programme under grant agreement No 646039. This work was supported by the European Commission under project FLEXITRANSTORE – H2020-LCE-2016-2017-SGS-774407.

References

[1] United Nations. Framework Convention on Climate Change, http://unfccc.int/kyoto_protocol/items/2830.php.
[2] RE100. http://there100.org/.
[3] Pineda S, Conejo AJ. Managing the financial risks of electricity producers using options. Energy Econ 2012;34(6):2216–27.
[4] OMIE. Operador del Mercado Ibérico de Electricidad (OMIE), http://www.omie.es/en/inicio.
[5] IRENA. International Renewable Energy Agency, https://www.irena.org/energytransition.
[6] Hu J, Xu Y, Cheng KW, Guerrero JM. A model predictive control strategy of pv-battery microgrid under variable power generations and load conditions. Appl Energy 2018;221:195–203.
[7] Sardi J, Mithulananthan N, Hung DQ. Strategic allocation of community energy storage in a residential system with rooftop pv units. Appl Energy 2017;206:159–71.
[8] Iria J, Soares F, Matos M. Optimal bidding strategy for an aggregator of prosumers in energy and secondary reserve markets. Appl Energy 2019;238:1361–72.
[9] Mouli GC, Bauer P, Zeman M. System design for a solar powered electric vehicle charging station for workplaces. Appl Energy 2016;168:434–43.
[10] Nguyen S, Peng W, Sokolowski P, Alahakoon D, Yu X. Optimizing rooftop photovoltaic distributed generation with battery storage for peer-to-peer energy trading. Appl Energy 2018;228:2567–80.
[11] Muñoz JI, de la Nieta AAS, Contreras J, Bernal-Agustín JL. Optimal investment portfolio in renewable energy: The Spanish case. Energy Policy 2009;37(12):5273–84.
[12] Dobrotkova Z, Surana K, Audinet P. The price of solar energy: Comparing competitive auctions for utility-scale solar pv in developing countries. Energy policy 2018;118:133–48.
[13] de la Nieta AAS, Martins RFM, Tavares TAM, Matias JCO, Catalão JPS, Contreras J. Short-term trading for a photovoltaic power producer in electricity markets. 2015 IEEE power & energy society general meeting. IEEE; 2015. p. 1–5.
[14] Comello S, Reichelstein S, Sahoo A. The road ahead for solar pv power. Renew Sustain Energy Rev 2018;92:744–56.
[15] McConnell D, Hearps P, Eales D, Sandiford M, Dunn R, Wright M, et al. Retrospective modeling of the merit-order effect on wholesale electricity prices from distributed photovoltaic generation in the Australian national electricity market. Energy Policy 2013;58:17–27.
[16] Cludius J, Hermann H, Matthes FC, Graichen V. The merit order effect of wind and photovoltaic electricity generation in Germany 2008–2016: Estimation and distributional implications. Energy Econ 2014;44:302–13.
[17] Tveten ÅG, Bolkesjø TF, Martinsen T, Hvarnes H. Solar feed-in tariffs and the merit order effect: A study of the German electricity market. Energy Policy 2013;61:761–70.
[18] Ye LC, Rodrigues JFD, Lin HX. Analysis of feed-in tariff policies for solar photovoltaic in China 2011–2016. Appl Energy 2017;203:496–505.
[19] Hsu CW. Using a system dynamics model to assess the effects of capital subsidies and feed-in tariffs on solar pv installations. Appl Energy 2012;100:205–17.
[20] Zhang Q, Wang G, Li Y, Li H, McLellan B, Chen S. Substitution effect of renewable portfolio standards and renewable energy certificate trading for feed-in tariff. Appl Energy 2018;227:426–35.
[21] Zwaenepoel B, Laveyne JI, Vandevelde L, Vandoorn TL, Meersman B, Van Eetvelde G. Solar commercial virtual power plant. 2013 IEEE power & energy society general meeting. IEEE; 2013. p. 1–5.
[22] Xiao D, Qiao W, Qu L. Risk-averse offer strategy of a photovoltaic solar power plant with virtual bidding in electricity markets. 2019 IEEE Power & Energy Society Innovative Smart Grid Technologies Conference (ISGT). IEEE; 2019. p. 1–5.
[23] Saranya A, Swarup KS. Offering strategy for a photovoltaic power plant in electricity market. 2018 IEEE Power and Energy Conference at Illinois (PECI). IEEE; 2018. p. 1–6.
[24] Morales JM, Conejo AJ, Pérez-Ruiz J. Short-term trading for a wind power producer. IEEE Trans Power Syst 2010;25(1):554–64.
[25] de la Nieta AAS, Contreras J, Muñoz JI. Optimal coordinated wind-hydro bidding strategies in day-ahead markets. IEEE Trans Power Syst 2013;28(2):798–809.
[26] de la Nieta AAS, Contreras J, Muñoz JI, Catalão JaP. Optimal wind reversible hydro offering strategies for midterm planning. IEEE Trans Sustainable Energy 2015;6(4):1356–66.
[27] Uryasev S. Conditional value-at-risk: Optimization algorithms and applications. In: Proceedings of the IEEE/IAFE/INFORMS 2000 Conference on Computational Intelligence for Financial Engineering (CIFEr) (Cat. No. 00TH8520), IEEE; 2000, p. 49–57.
[28] de la Nieta AAS, Martins RF, Catalão JP, Contreras J. Optimal coordinated wind-photovoltaic bidding in electricity markets. 2015 Australasian Universities Power Engineering Conference (AUPEC). IEEE; 2015. p. 1–6.
[29] Díaz G, Coto J, Gómez-Aleixandre J. Optimal operation value of combined wind power and energy storage in multi-stage electricity markets. Appl Energy 2019;235:1153–68.
[30] Ding H, Hu Z, Song Y. Rolling optimization of wind farm and energy storage system in electricity markets. IEEE Trans Power Syst 2015;30(5):2676–84.
[31] Faria P, Spínola J, Vale Z. Reschedule of distributed energy resources by an aggregator for market participation. Energies 2018;11(4):713.
[32] Davidson C, Steinberg D, Margolis R. Exploring the market for third-party-owned residential photovoltaic systems: insights from lease and power-purchase agreement contract structures and costs in california. Environ Res Lett 2015;10(2):024006.
[33] de la Nieta AAS, Contreras J, Catalão JP. Optimal single wind hydro-pump storage bidding in day-ahead markets including bilateral contracts. IEEE Trans Sustainable Energy 2016;7(3):1284–94.
[34] Spinler S, Huchzermeier A, Kleindorfer P. Risk hedging via options contracts for physical delivery. Or Spectrum 2003;25(3):379–95.
[35] Oum Y, Oren S, Deng S. Hedging quantity risks with standard power options in a competitive wholesale electricity market. Naval Res Logist (NRL) 2006;53(7):697–712.
[36] Nikkinen J, Rothovius T. Market specific seasonal trading behavior in NASDAQ OMX electricity options. J Commodity Mark 2019;13:16–29.
[37] Carmichael DG. Energy options. Future-proofing—Valuing adaptability, flexibility, convertibility and options. Springer; 2020. p. 149–53.
[38] Papakonstantinou A, Champeri G, Delikaraoglou S, Pinson P. Trading wind power through physically settled options and short-term electricity markets. Wind Energy 2019;22(11):1487–99.
[39] Crespo-Vazquez JL, Carrillo C, Diaz-Dorado E, Martinez-Lorenzo JA, Noor-E-Alam M. A machine learning based stochastic optimization framework for a wind and storage power plant participating in energy pool market. Appl Energy 2018;232:341–57.
[40] Skajaa A, Edlund K, Morales JM. Intraday trading of wind energy. IEEE Trans Power Syst 2015;30(6):3181–9.

[41] Bertrand G, Papavasiliou A. Adaptive trading in continuous intraday electricity markets for a storage unit. IEEE Trans Power Syst 2019:1. https://doi.org/10.1109/TPWRS.2019.2957246.
[42] Koch C, Hirth L. Short-term electricity trading for system balancing: An empirical analysis of the role of intraday trading in balancing germany's electricity system. Renew Sustain Energy Rev 2019;113:109275.
[43] González-Garrido A, Saez-de-Ibarra A, Gaztañaga H, Milo A, Eguia P. Annual optimized bidding and operation strategy in energy and secondary reserve markets for solar plants with storage systems. IEEE Trans Power Syst 2019;34(6):5115–24.
[44] Perez E, Beltran H, Aparicio N, Rodriguez P. Predictive power control for pv plants with energy storage. IEEE Trans Sustainable Energy 2012;4(2):482–90.
[45] PCR & EUPHEMIA algorithm, the European Power Exchange project to couple electricity market, https://www.n-side.com/pcr-euphemia-algorithm-european-power-exchanges-price-coupling-electricity-market/.
[46] REE. Red Elélectrica de España (REE), http://www.ree.es/en.
[47] esios. System of information of the market system operator, https://www.esios.ree.es/en.
[48] AEMET. http://meteo.navarra.es/estaciones/estacion.cfm?IDestacion=405.
[49] Conejo AJ, Carrion M, Morales JM. Decision making under uncertainty in electricity markets. Springer; 2010.
[50] Vagropoulos SI, Kardakos EG, Simoglou CK, Bakirtzis AG, Catalão JPS. ANN-based scenario generation methodology for stochastic variables of electric power systems. Electric Power Syst Res 2016;134:9–18.
[51] Breiman L. Random forests. Machine Learn 2001;45(1):5–32.